Asian Journal of Chemistry; Vol. 35, No. 1 (2023), 83-88

ASIAN JOURNAL OF CHEMISTRY

https://doi.org/10.14233/ajchem.2023.23999

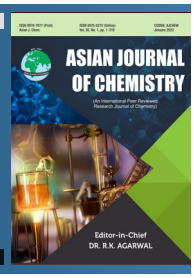

Synthesis and Morphological Studies of Nanocellulose Fibers from Lignocellulosic Biomass in Ionic Liquid

J.K. PRASANNAKUMAR[1,*], G.K. PRAKASH[2], B. SURESH[3], B.E. BASAVARAJAPPA[1], H.S. ONKARAPPA[4], BHARATH K. DEVENDRA[5] and S.G. PRASANNAKUMAR[5]

[1]Research Centre, Department of Chemistry, Bapuji Institute of Engineering and Technology (Affiliated to Visvesvaraya Technological University, Belagavi), Davangere-577004, India
[2]Department of Chemistry, Sri Taralubalu PU College, Davangere-577004, India
[3]Department of Civil Engineering, Bapuji Institute of Engineering and Technology (Affiliated to Visvesvaraya Technological University, Belagavi), Davangere-577006, India
[4]Department of Chemistry, G.M. Institute of Technology (Affiliated to Visvesvaraya Technological University, Belagavi), Davanagere-577006, India
[5]Department of Chemistry, M.S. Ramaiah College of Arts, Science and Commerce, MSR Nagar, MSRIT Post, Bengaluru-560054, India

*Corresponding author: Fax: +91 8192 223261; Tel: +91 8192 222245; E-mail: prassvin@gmail.com

Received: 26 July 2022; *Accepted*: 9 November 2022; *Published online*: 27 December 2022; AJC-21082

Lignocellulosic agricultural biomasses and wood are the two most important natural sources of cellulose available on the planet. When chemically treated, cellulose is the world's most common and widely used biopolymer, with properties such as low price, good toughness, good biocompatibility and good thermal stability. In this study, nanocellulose was extracted from ragi stalk, mango wood and groundnut husk. The cellulose was alkali-treated with NaOH and bleached with sodium chlorite to remove lignin and hemicellulose. Ionic liquid (1-butyl-3-methylimidazolium chloride ([Bmim]Cl) solvent was used to treat the obtained cellulose. FTIR spectra highlight the functional groups and substantial conversion of cellulose to nanocellulose. The crystalline or semi-crystalline nature of synthesized nanocellulose was illustrated by XRD. The TEM images record the size of synthesized nanocellulose between 11.12 and 31.16 nm. The reduction in size is mainly due to ultrasonication and centrifugation. The thermal stability of the obtained nanocellulose was evidenced using TGA/DTA. The thermal studies insight that the synthesized nanocellulose samples possess superior degradation temperature up to 473.8 ºC.

Keywords: Ragi stalk, Mango wood, Groundnut husk, Ionic liquid, Nanocellulose.

INTRODUCTION

The energy sectors around the world are facing challenges to meet the demand and supply gap of energy as a result of population growth and industrial globalization. After coal and oil, biomass, a carbon-neutral renewable resource derived from the carbon containing waste of diverse natural and anthropogenic processes, has emerged as the third primary energy resource to close the energy gap [1]. Biomass could be generated from a variety of sources, including the timber industry besides, agriculture sector crops, forest raw materials, significant parts of domestic wastes and wood. As a result, researchers and developers are increasing their focus aside from coal and oil and toward biomass, which will not only produce carbon-neutral energy but also solve a range of problems such as management of solid waste, health implications and bushfires [2].

As a developing nation, India has battled for decades to comply with global environmental and solid-waste management norms, which has been a significant obstacle. It generates an annual average of 960-1000 million tonnes of solid waste, with the agricultural sector accounting for a large portion of this [3]. Post-harvesting is responsible for about 13% of all solid wastes produced in Asia [4]. India tops the third position in the globe to grow maize, paddy and wheat, so researchers are most interested in how to use the type of cellulose that comes from these crops. The most under-utilized forms of cellulose, are ragi stalk, mango wood and groundnut husk [5,6]. With 50% of the workforce employed in agriculture. Natural cellu-

lose is self-sufficient in India and there is a large amount of biowastes. Countries such as the United States, Europe, Canada and Australia prioritize nanocellulose production due to its application as a commercial product [7-9].

Cellulose and lignocellulose nanoparticles play a vital role in nanotechnology. In terms of nature, size and function, nanocellulose is largely dependent on its parent cellulose. Moreover, cellulose is a multipurpose raw material that can replace a number of non-renewable substances [10]. Cellulose nanocrystals (CNCs) and cellulose nanofibrils are the two major types of cellulose nanomaterials that can be derived from a variety of plant and animal sources (CNFs). Depending on their size and extraction process, cellulose nanocrystals may be referred to as cellulose nanowhiskers (CNW) or nanocrystalline cellulose (NCC) [11,12] and cellulose nanofibrils may be referred to as nanofibrillated cellulose (NFC) or microfibrillated cellulose (MFC) [13].

Ragi stalk and groundnut husk are found to be soft materials and the average length of the ragi stalk is 0.5 m when compared to other sources. Due to its lower lignin content (5-6%) and shorter growing cycle (~ 80 days), ragi stalk (finger millet) is widely suggested as a superior starting material for nanocellulose production [14,15]. Because of its shorter length and growing cycle of 60-100 days, the groundnut husk also follows ragi stalk. On the other hand, mango wood has a porous anisotropic structure, which gives a unique combination of high strength, stiffness and thinness. For the extraction of cellulose and nanocellulose, numerous plants, such as husk of coconut rice and maize, hemp, sisal, flax, sugar cane bagasse, *etc.*, have been studied [16]. Ragi stalk, mango wood and groundnut husk are therefore strongly suggested for the synthesis of nanocellulose, taking into account the availability of raw materials as well as their feasibility.

Two common processes have been developed for nanocellulose synthesis *viz.* the chemical method, which involves the acid hydrolysis of nanocellulose and the oxidation method, which uses TEMPO (2,2,6,6-tetramethyperidine-1-oxyl). Due to its diverse features, availability and flexibility in reuse, the ionic liquid approach has been replacing these conventional methods in recent years. Naturally occurring cellulose is insoluble in the majority of solvents, however, it is soluble in ionic liquids [17]. The common ionic liquids for dissolving cellulose include 1-butyl-3-methylimidazolium chloride (BmimCl), 1-allyl-3-methylimidazolium chloride (AmimCl) and 1-ethyl-3-methylimidazole acetate [18]. Recent studies have identified ionic liquids as suitable solvents, swelling agents and catalysts for nanocellulose synthesis. The major benefit of employing ionic liquid as a pretreatment is the reproducibility of insolvency recovery with minimum loss. It has been established that more than 90% of BmimCl's activity can be recovered by reusing it four times without losing its potency [19]. The use of ionic liquid as a nanocellulose surface modification medium has applications in nanomedicine and drug delivery [20]. Ionic liquid has recently been recommended as a reaction media for the homogenous production of cellulose. Therefore, according to some researchers, homogeneous cellulose acetylation can be accomplished in AmimCl without the need for catalysts, resulting in cellulose acetates with a wide range of substitution degrees [21]. Moreover, ionic acids does not offer acid waste and said to be greener pathway in isolating nanocellulose compared to the conventional methods [22]. The purpose of this study is to synthesize nanocellulose from ragi Stalk, mango wood and groundnut husk and to compare their prop-erties using an ionic liquid. The FT-IR, XRD, SEM, TEM and TGA/DTA techniques were used to examine the effects of ionic liquid on dissolution, morphology, thermal stability, crystall-inity and size in all three cellulosic materials.

EXPERIMENTAL

The lignocellulosic materials such as ragi stalk, mango wood and groundnut husk were collected from farmlands in and around Davanagere city, India. The chemicals *viz*. chlorobutane and 1-methylimidazole were bought from Sigma- Aldrich, India, while others like $NaClO_2$, NaOH and CH_3COOH were purchased from Merck and Qualigens. All chemicals have a purity of 98 to 99% and were used as such without purification.

Alkali treatment: Finely ground, sieved ragi stalk, mango wood and groundnut husk powders (10 g each) were treated individually with a 5% NaOH solution for 2 h at temperatures ranging from 85 to 100 ºC to remove hemicellulose. The obtained mass was filtered by repeated rinsing with distilled water until it reached a pH of 7. After that, the product was oven-dried for a day or until it reaches a constant weight. This process makes fibres more susceptible to bleaching, acid hydrolysis and chemical modification.

Bleaching treatment: After being treated with alkali, the samples were bleached to remove any remaining lignin. Alkali-treated samples were treated with 5% sodium chlorite solution and then the mixture was refluxed using a thermomagnetic stirrer between 85-110 ºC for 3-4 h by dropwise addition of acetic acid to maintain acidic medium. Repetitive washing with distilled water eliminated the residual lignin and the synthesized cellulose was filtered by deionized water washing until it reached a neutral pH. The obtained mass was oven-dried for one day or till it yields constant weight and stored for further process.

Synthesis of nanocellulose in ionic liquid: Ragi stalk nanocellulose (IL-RSNC), mango wood nanocellulose (IL-MWNC) and groundnut husk nanocellulose (IL-GHNC) were synthesized separately by adding 10 g of 1-butyl-3-methyl-imidazolium chloride (IL) into a 100 mL dry two necked flask fitted with a water-cooled condenser carries calcium guard tube at the outlet and placed in an oil bath. In brief, 1 g of dried and finely ground ragi stalk cellulose (RSC), mango wood cellulose (MWC) and groundnut husk cellulose (GHC) were added individually and slowly into the flask containing the ionic liquid and refluxed on a thermomagnetic stirrer at 115 to 120 ºC for 1-2 h. Upon dissolution of cellulose, a pale yellow solution was obtained and then appeased by adding 50 mL of ice-cold distilled water. The resulting nanocellulose precipitate was filtered and washed 5-6 times with cold distilled water followed by ultrasonication for 45 min and centrifugation under 2000 rpm for 30 min. The reaction mass was dried and stored.

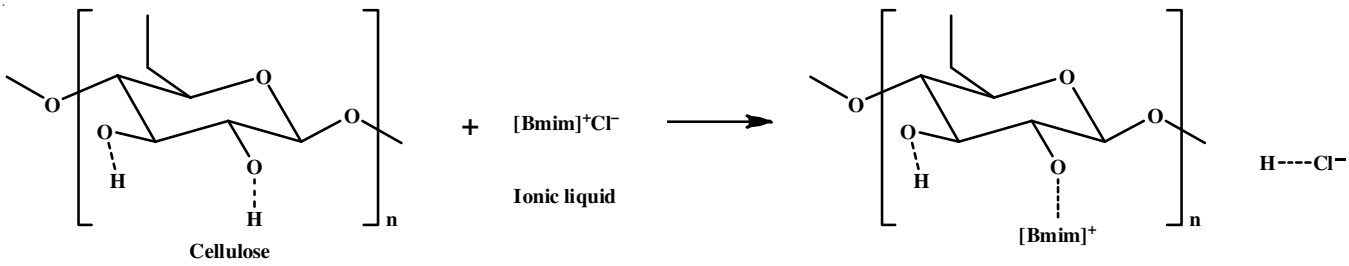

Fig. 1. Dissolution of cellulose with ionic liquid

Characterization: The FTIR of cellulose, IL-RSNC, IL-MWNC and IL-GHNC were recorded using Thermo Nicolet iS50 FTIR spectrophotometer using KBr method in the range of 4000-400 cm^{-1}. The XRD data were recorded using a Bruker D8 advance diffractometer. The crystalline and amorphous zone peak heights were measured and the crystallinity index (CI) was calculated using Scherrer's formula with a 0.02 step size. A Jeol 6390LA/OXFORD XMX N instrument was used to capture SEM images with an acceleration voltage range of 0.5 to 30 kV. A secondary electron (SE) detector was used to acquire the images. TEM images were recorded using a 200 kV, LaB6 electron gun with a 0.23 nm point resolution and 0.14 nm lattice resolution. The thermogravimetric analysis (TGA and DTA) were performed using the Perkin-Elmer STA 6000 instrument.

RESULTS AND DISCUSSION

Fig. 1 depicts the representative cellulose dissolution mechanism in which the cation of the ionic liquid interacts favourably *via* hydrogen bonding with the hydroxyl protons of cellulose, breaking the strong intermolecular hydrogen bonds between carbohydrate chains and promoting dissolution [23-27].

FTIR analysis: The FTIR of IL-RSNC, IL-MWNC and IL-GHNC spectra is shown in Fig. 2. All four types of cellulose will have similar cellulose-I structured absorption peaks between 3321.59 and 3332.35 cm^{-1}, owing to -OH stretching vibrations caused by hydrogen bonding. The peaks in 2892.52-2901.02 cm^{-1} region denote the C-H stretching vibrations whereas, the peaks between 1636.04 and 1641.23 cm^{-1} are attributed to the H-O-H deformation of absorbed water and conjugated C=O stretch vibrations. The region of absorption between 1390 and 1428.27 cm^{-1} was attributed to asymmetric C-H deformation, which shifted to a low wavenumber and became weaker due to a reaction at higher temperatures with ionic liquid. The breaking of H-bonding at O-6 and the C-O antisymmetric bridge stret-ching is represented by the peak in the range 1157.25 to 1161.34 cm^{-1}. The C-O-C pyranose ring skeletal vibration was assigned peaks ranging from 1029.99 to 1066.28 cm^{-1}. In cellulose, the peak at 897.09 cm^{-1} is correlated to the glycosidic linkage and disappeared in nanocellulose indicating that there is an efficient transformation. Absorption peaks moving to the higher wave-numbers showed an efficient transition from cellulose I to cellulose II. This result shows that there was no other reaction in the middle of the dissolving process.

XRD analysis: Fig. 3 shows the X-ray diffraction patterns of IL-RSNC, IL-MWNC and IL-GHNC were treated with an

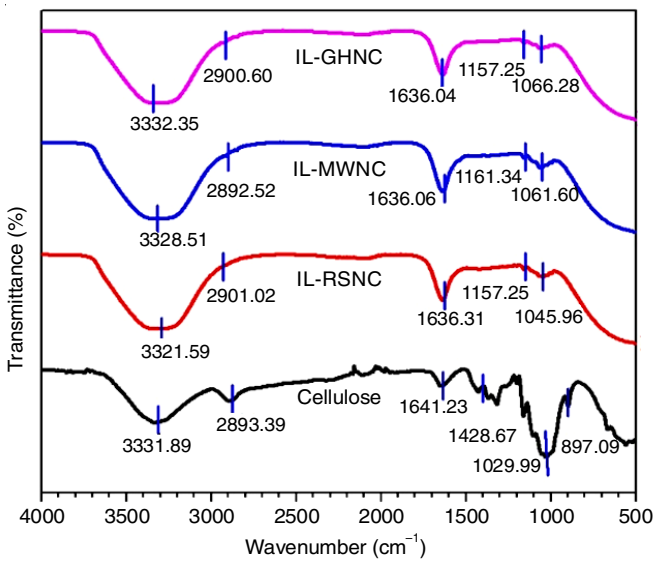

Fig. 2. FTIR of cellulose, IL-RSNC, IL-MWNC and IL-GHNC

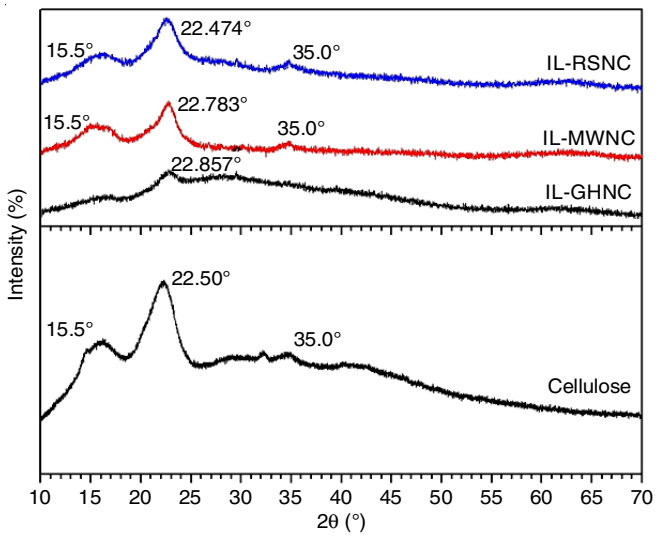

Fig. 3. XRD pattern of IL-RSNC, IL-MWNC, IL-GHNC and cellulose

ionic liquid and cellulose. These XRD patterns depict the semi-crystalline materials with an amorphous wide hump and crystalline peaks. The IL-RSNC exhibits its 2θ values in the range between 15.50º, 22.474º and 35.0º, IL-MWNC shows peaks at 15.50º, 22.783º and 35.0º, IL-GHNC exhibits the peaks in the range between 15.50º, 22.857º and cellulose shows the peak at 15.50º, 22.85º and 35.0º. Due to the disruption of intermolecular and intramolecular hydrogen bonds of cellulose by the

ionic liquid and ultrasonication, the crystallinity index of the synthesized nanocellulose is reported to be slightly lower than that of cellulose. The decrease in the crystallinity is due to the more complete dissolution of cellulose in ionic liquid.

SEM analysis: Prepared nanocellulose was found to be fibrous with considerable aggregation as seen by SEM images (Fig. 4). The surface morphology depicts the nanoscale dimensions, including uneven cross-sections, lumens and a vast number of microscopic microfibrils, as well as various forms and non-uniform surfaces. Fig. 4a-b show the morphology of IL-RSNC corresponds to nanosized fibres in the form of regular structured bundles. The morphology of IL-MWNC corresponding to the surface of fibres is shown in Fig. 4c-d, indicating that clusters of individualized fibres can be observed on the surface and that the reduction of fibre diameters is more visible. Fig. 4e-f show the morphology of IL-GHNC corresponds to the cluster-like nanofibers with smooth surfaces. Here, individualized nanofibers can be obtained with ultrasonic treatment. The average size of the ionic liquid-assisted synthesized nanocellulose was found to be in the range of nanoscale.

TEM analysis: The TEM images of IL-RSNC (a & b), IL-MWNC (b & c) and IL-GHNC (e & f) were obtained to analyze the internal morphology and structure of the synthesized nanocellulose as shown in Fig. 5. In accordance with the TEM images, the synthesised nanocellulose was in the form of discrete, bundled, fibrillar and easily observable nanofibers. Even the tendency to agglomerate can be seen in all of the images. The IL-RSNC demonstrates that the regularly structured nanofibers have an average size between 14.58 and 22.17 nm. The average diameter of IL-MWNC fibres ranges from 27.33 to 34.85 nm, whereas IL-GHNC reveals the formation of nanofibers with an average diameter between 11.72 and 31.16 nm. It was inferred that the synthesized nanocellulose well exhibits the nanoscale dimensions. The structured nanofiber can be seen in IL-RSNC, IL-MWNC exhibits nanofibers with a narrow distribution, while IL-GHNC shows the nanofibers with a less dispersed size distribution. The above analysis reveals that the ionic liquid readily dissolves the cellulose, which affects the structure and morphology and size distribution of synthesized nanocellulose.

Thermal studies: The thermal stability of IL-RSNC, IL-MWNC and IL-GHNC was examined by using TGA and the DTA curves are shown in Figs. 6 and 7, respectively. The water evaporation in all the synthesized nanocellulose was observed between 109 and 145.9 ºC. The degradation temperature of IL-RSNC is 329.5, 443.1 and 459.9 ºC and the degradation temperature of IL-MWNC was 250.1, 458.4 and 473.8 ºC, whereas the degradation temperature of IL-GHNC was 327.4 ºC and 467.0 ºC, respectively. The depolymerization of hemicellulose and glycosidic links, which have broken, is shown by the significant weight loss between 250.0 and 329.5 ºC regions. The onset degradation temperature was found to be 330 ºC. Here, the weight loss occurred in three stages, the first stage was associated with evaporation of water the second and third stages of weight loss occurred in the range 327.4 to 473.8 ºC. The results demonstrated that the produced nanocellulose demonstrates higher heat stability after being IL-treated between 459.9 and 473.8 ºC.

Conclusion

In this work, a lignocellulosic agricultural biomass derived from ragi (finger millet) stalk, mango wood and groundnut husk were used to synthesize nanocellulose in an ionic liquid. The FTIR spectra suggested that the ionic liquid treated lignocellulosic biomass *viz*. IL-RSNC, IL-MWNC and IL-GHNC exhibit

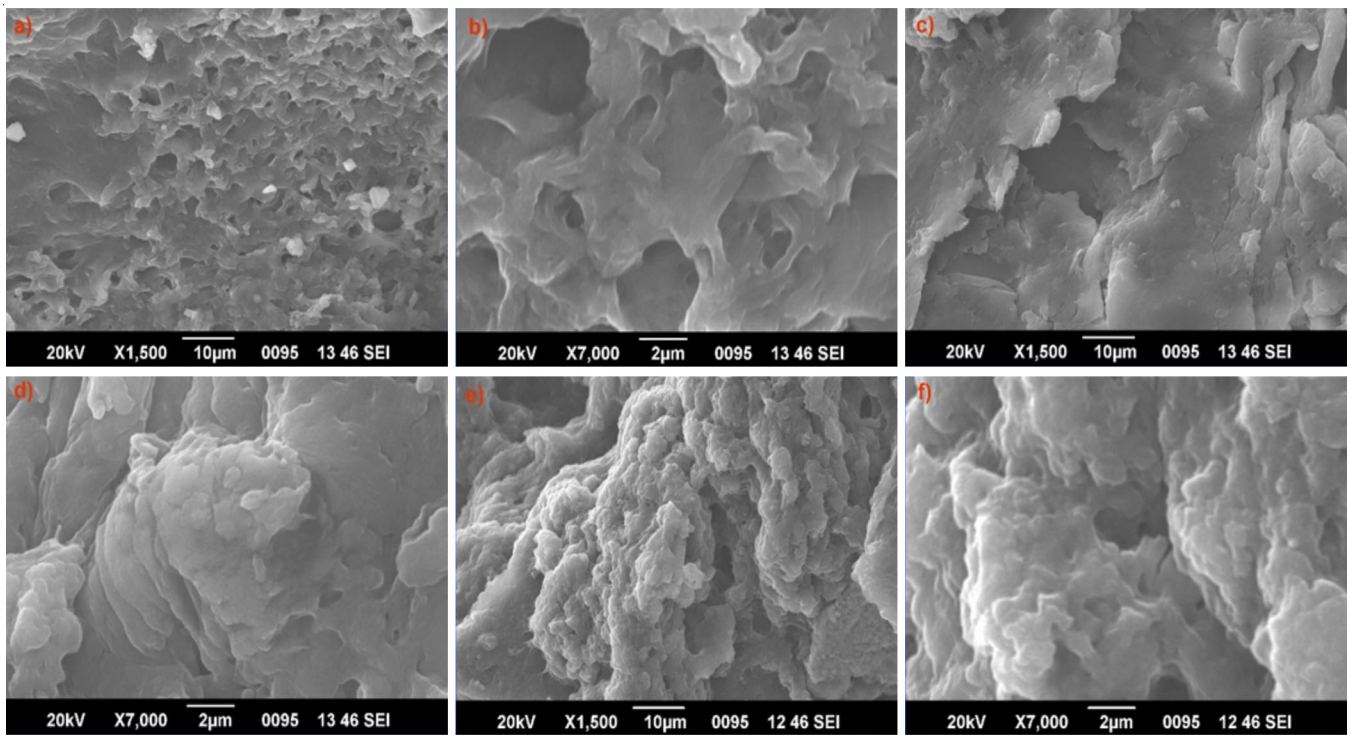

Fig. 4. SEM of (a) & (b): IL-RSNC, (c) & (d): IL-MWNC and (e) & (f): IL-GHNC

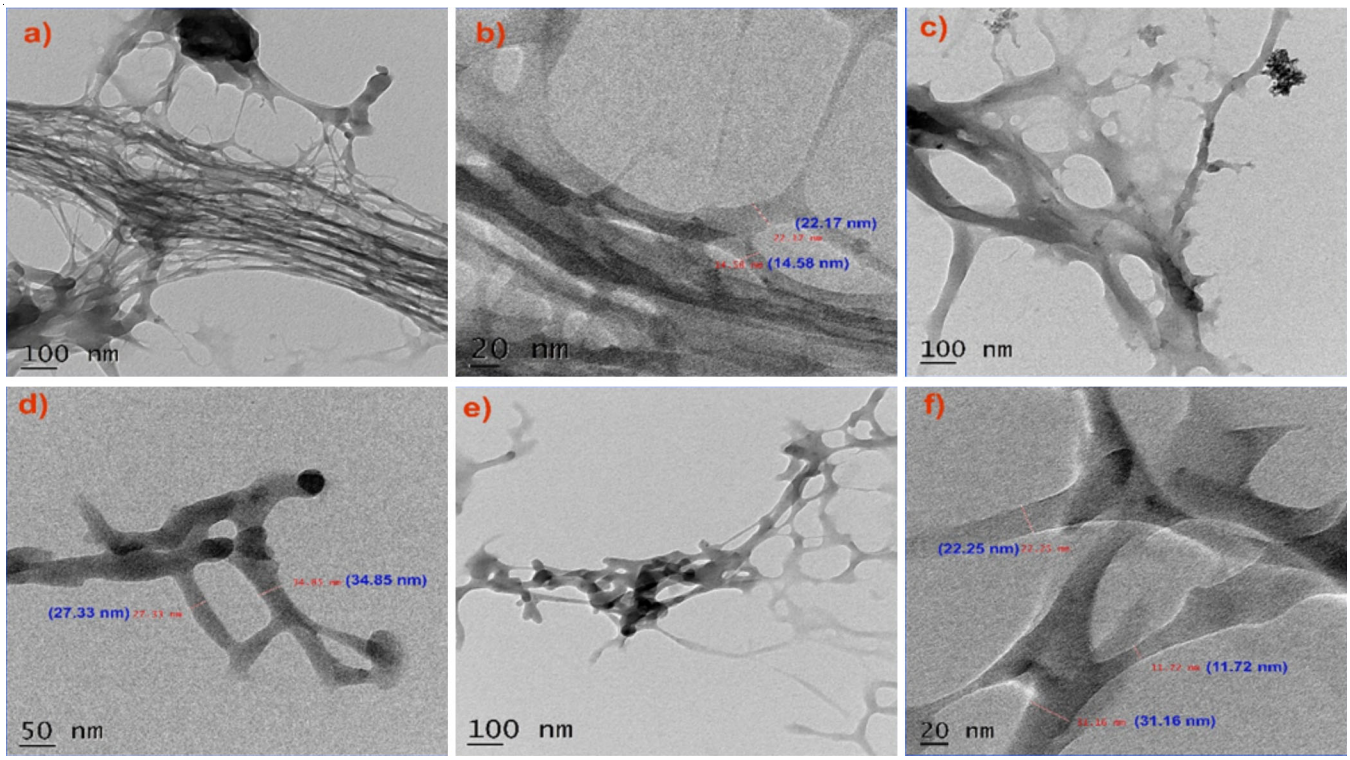

Fig. 5. TEM of (a & b)-IL-RSNC, (c & d)-IL-MWNC and, (e & f)-IL-GHNC

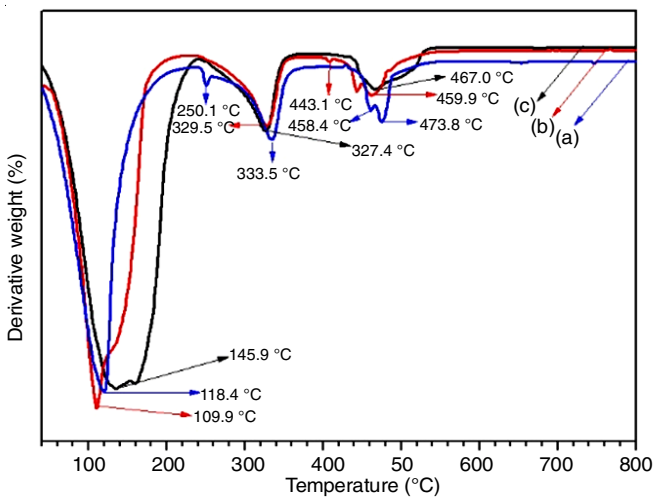

Fig. 6. TGA of a) IL-GHNC (black), b) IL-MWNC (blue) and c) IL-RSNC (red)

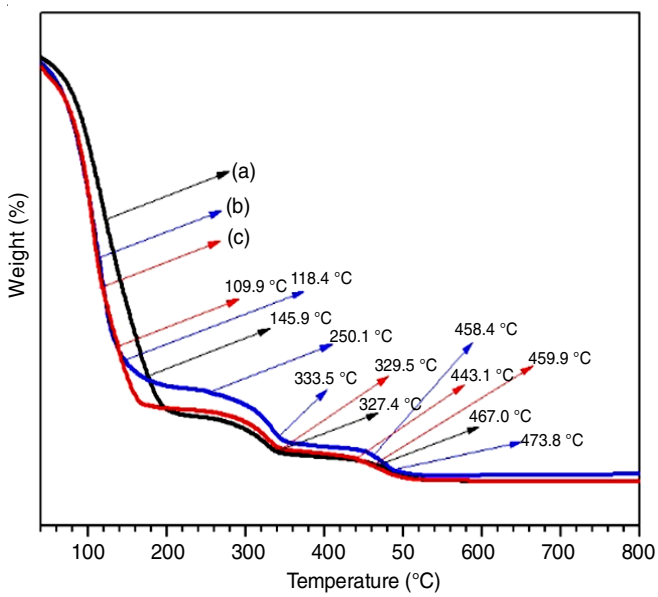

Fig. 7. DTG of (a) IL-GHNC (Black), (b) IL-MWNC (blue) and (c) IL-RSNC (red)

the same distinctive cellulose peaks, thus confirmed that no derivational reaction was occured during the cellulose dissolution process. According to X-ray crystallographic investigations, the synthesized nanocellulose consists of semi-crystalline materials with an amorphous wide hump and crystalline peaks. It implies that the hydrogen bonds of cellulose were disrupted, resulting in the disintegration of the crystal structure during the entire process. Different shapes with a non-uniform surface, regular cross-sections and a great number of microscopic microfibrils were observed in the SEM images. The TEM images showed that the cellulose synthesized is in the nanoscale dimension. According to TGA/DTA analysis, the strong troughs in the DTA curve revealed that the onset of the breakdown of ionic liquid treated cellulose was ~335 ºC. The IL-RSNC, IL-MWNC and IL-GHNC have shown higher thermal stability. TGA revealed that ionic liquid treated MWNC has a higher degradation temperature (473.8 ºC), indicating greater thermal stability. Furthermore, this research seeks to demonstrate the remarkable practical applications of synthesized nanocellulose from agricultural biomass, which will undoubtedly meet India's need for solid waste management and reduce chemical waste through a more realistic approach to nanocellulose manufacturing.

ACKNOWLEDGEMENTS

The authors are thankful to the Management, Director, Principal of Bapuji Institute of Engineering and Technology, Davanagere. The authors are grateful to the Head of the Sophisticated Test and Instrumentation Centre (STIC), Cochin for having provided the analysis data.

CONFLICT OF INTEREST

The authors declare that there is no conflict of interests regarding the publication of this article.

REFERENCES

1. P.A. Owusu and S. Asumadu-Sarkodie, *Cogent Eng.*, **3**, 1167990 (2016); https://doi.org/10.1080/23311916.2016.1167990
2. B. Sharma and B. Mohanty, *RSC Adv.*, **11**, 13396 (2021); https://doi.org/10.1039/D1RA01467F
3. V.D. Katare and M.V. Madurwar, *Constr. Build. Mater.*, **152**, 1 (2017); https://doi.org/10.1016/j.conbuildmat.2017.06.142
4. M. Duque-Acevedo, L.J. Belmonte-Ureña, F.J. Cortés-García and F. Camacho-Ferre, *Glob. Ecol. Conserv.*, **22**, e00902 (2020); https://doi.org/10.1016/j.gecco.2020.e00902
5. P. Jagadesh, A. Ramachandramurthy and R. Murugesan, *Constr. Build. Mater.*, **176**, 608 (2018); https://doi.org/10.1016/j.conbuildmat.2018.05.037
6. N. Reddy and Y. Yang, *Green Chem.*, **7**, 190 (2005); https://doi.org/10.1039/b415102j
7. N. Lin and A. Dufresne, *Eur. Polym. J.*, **59**, 302 (2014); https://doi.org/10.1016/j.eurpolymj.2014.07.025
8. T. Abitbol, A. Rivkin, Y. Cao, Y. Nevo, E. Abraham, T. Ben-Shalom, S. Lapidot and O. Shoseyov, *Curr. Opin. Biotechnol.*, **39**, 76 (2016); https://doi.org/10.1016/j.copbio.2016.01.002
9. D. Klemm, F. Kramer, S. Moritz, T. Lindström, M. Ankerfors, D. Gray and A. Dorris, *Angew. Chem. Int. Ed.*, **50**, 5438 (2011); https://doi.org/10.1002/anie.201001273
10. T.H. Wegner and P.E. Jones, *Cellulose*, **13**, 115 (2006); https://doi.org/10.1007/s10570-006-9056-1
11. E. Fortunati, D. Puglia, M. Monti, L. Peponi, C. Santulli, J.M. Kenny and L. Torre, *J. Polym. Environ.*, **21**, 319 (2013); https://doi.org/10.1007/s10924-012-0543-1
12. H. Dong, J.F. Snyder, D.T. Tran and J.L. Leadore, *Carbohydr. Polym.*, **95**, 760 (2013); https://doi.org/10.1016/j.carbpol.2013.03.041
13. A. Bledzki, *Prog. Polym. Sci.*, **24**, 221 (1999); https://doi.org/10.1016/S0079-6700(98)00018-5
14. P.K.J. Kallappa, P.G. Kalleshappa, S. Basavarajappa and B.B. Eshwarappa, *Asian J. Green Chem.*, **3**, 273 (2022); https://doi.org/10.22034/ajgc.2022.3.7
15. M.V.S.S.T. Subba Rao and G. Muralikrishna, *J. Agric. Food Chem.*, **54**, 2342 (2006); https://doi.org/10.1021/jf058144q
16. C.A.D.C. Mendes, F.A.D.O. Adnet, M.C.A.M. Leite, C.G. Furtado and A.M.F.D. Sousa, *Cellul. Chem. Technol.*, **49**, 727 (2015).
17. N. Mohd, S.F.S. Draman, M.S.N. Salleh and N.B. Yusof, *AIP Conf. Proc.*, **1809**, 020035 (2017); https://doi.org/10.1063/1.4975450
18. M. Babicka, M. WoŸniak, K. Szentner, M. Bartkowiak, B. Pepliñska, K. Dwiecki, S. Borysiak and I. Ratajczak, *Materials*, **14**, 3264 (2021); https://doi.org/10.3390/ma14123264
19. P. Phanthong, S. Karnjanakom, P. Reubroycharoen, X. Hao, A. Abudula and G. Guan, *Cellulose*, **24**, 2083 (2017); https://doi.org/10.1007/s10570-017-1238-5
20. G.A.S. Haron, H. Mahmood, M.H. Noh, M.Z. Alam and M. Moniruzzaman, *ACS Sustain. Chem. Eng.*, **9**, 1008 (2021); https://doi.org/10.1021/acssuschemeng.0c06409
21. M.B. Turner, S.K. Spear, J.D. Holbrey and R.D. Rogers, *Biomacromolecules*, **5**, 1379 (2004); https://doi.org/10.1021/bm049748q
22. N. Pal, H. Hoteit and A. Mandal, *J. Mol. Liq.*, **339**, 116811 (2021); https://doi.org/10.1016/j.molliq.2021.116811
23. O.A. El-Seoud, M. Kostag, K. Jedvert and N.I. Malek, *Polymers*, **11**, 1917 (2019); https://doi.org/10.3390/polym11121917
24. J.H. Poplin, R.P. Swatloski, J.D. Holbrey, S.K. Spear, A. Metlen, M. Grätzel and R.D. Rogers, *Chem. Commun.*, 2025 (2007); https://doi.org/10.1039/B704651K
25. B. Lindman, B. Medronho, L. Alves, C. Costa, H. Edlund and M. Norgren, *Phys. Chem. Chem. Phys.*, **19**, 23704 (2017); https://doi.org/10.1039/C7CP02409F
26. H. Wang, G. Gurau and R.D. Rogers, *Chem. Soc. Rev.*, **41**, 1519 (2012); https://doi.org/10.1039/C2CS15311D
27. R.C. Remsing, R.P. Swatloski, R.D. Rogers and G. Moyna, *Chem. Commun.*, **12**, 1271 (2006); https://doi.org/10.1039/b600586c